The Indiana University Proton Radiation Therapy Project

C. Bloch,[*] V. Derenchuk,[†] J. Cameron,[†] M. Fasano,[*] J. Gilmore,[‡] R. Hashemian,[**]
N. Hornback,[*] D.A. Low,[††] J. Morphis,[*] C. Peterson,[‡‡] D. Rosselot,[*] G. Sandison,[*] R-N. Shen,[*]
and H. Shidnia,[*]

[*]*Department of Radiation Oncology, Indiana University School of Medicine, Indianapolis, IN 46202*

[†]*Indiana University Cyclotron Facility, Indiana University, Bloomington, IN 47408*

[‡]*Department Nuclear Engineering, Massachusetts Institute of Technology, Cambridge, MA 02139*

[**]*Radiation Therapy, Bloomington Hospital, Bloomington, IN 47404*

[††]*Department of Radiation Oncology, Mallinckrodt Institute of Radiology, St. Louis, MO 63110*

[‡‡]*Department of Physics, La Sierra University, Riverside, CA 92515*

ABSTRACT

A fixed horizontal beam line at the Indiana University Cyclotron Facility (IUCF) has been equipped for proton radiation therapy treatment of head, neck, and brain tumors. The complete system will be commissioned and ready to treat patients by December of 1992. IUCF can produce external proton beams from 45 to 200 MeV in energy, which corresponds to a maximum range in water of 26 cm. Beam currents over 100 nA are easily attained, allowing dose rates in excess of 200 cGy/min, even for large fields. Beam spreading systems have been tested which provide uniform fields up to 20 cm in diameter. Range modulation is accomplished with a rotating acrylic device, which provides uniform depth dose distributions from 3 to 18 cm in extent. Tests have been conducted on detectors which monitor the beam position and current, and the dose symmetry. This report discusses those devices, as well as the cyclotron characteristics, measured beam properties, safety interlocks, computerized dose delivery/monitoring system, and future plans.

I. INTRODUCTION

The Indiana University Cyclotron Facility (IUCF) is an accelerator based research facility located on the Bloomington campus of Indiana University which receives most of its funding from the National Science Foundation's (NSF) nuclear physics budget. The development of a proton radiation therapy facility at IUCF, in collaboration with the Department of Radiation Oncology, has been facilitated by the availability of split beam which allows delivery of beam to two experiments.

The beam at IUCF has several key features that make it ideal for proton therapy. IUCF has a variable energy acceleration system which can produce beams of protons with energies from 45 to 200 MeV. However, more than one half of recent scheduled operation has been with proton beams in the energy range from 185 to 200 MeV, a range nearly ideal for the treatment of cancer. Unless otherwise specified, the remainder of this paper will assume beam in that energy range.

IUCF routinely delivers proton beams anywhere from 5 to 500 nA (or more) within a phase space area of about 2.5 π-mm-mr horizontal, by 2.0 π-mm-mr vertical. A new high intensity polarized ion source will soon improve this capability to 2 μA in the same phase space area. These high intensities allow us to easily provide dose rates of 200 cGy/min, even for the largest field size ($20\times20\times18$ cm^3). Finally, the time structure of the IUCF beam is essentially DC, which provides some technical advantages in any work that relies on rapid timing (e.g. raster scanning for treatments, proton radiography, or proton computed tomography).

II. IUCF

A method of splitting the beam from the cyclotron to two different beam lines using a fast switching magnet and Lambertson septum magnets has been in use at IUCF since 1986.[1] Typically a primary user receives a 90% duty factor while the secondary user receives the remaining 10%. The split period is adjustable, but is generally between 30 and 100 msec. Either user can, upon demand, receive 100% of the beam within the rise time limitations of the fast switching magnet. The peak beam intensity delivered to either user can be individually adjusted using a beam intensity modulation system timed to the period of the switching magnet. For proton therapy, initial set up and characterization of the beam before patient treatment can be completed as a secondary user, with little affect on the primary user. During the actual treatment, 100% of the beam would be required for up to 2 minutes. Impact on the nuclear physics research program will therefore be minimal.

Presently, there is no capability to split between the proton therapy beam line and the Cooler ring. At least 50% of cyclotron running time will be used to deliver beam to the Cooler ring, so upgrading the splitting system to allow a split between the Cooler and the proton therapy beam line is a high priority. Initial treatments will be scheduled to coincide with beam delivered to other areas of the lab.

III. PROTON THERAPY BEAM LINE

Layout of the proton therapy beam line with the beam spreading system, the range modulator and the beam and dose monitoring diagnostics are shown in Figure 1. The first item shown (starting upstream, shown as the left of Figure 1) is a multi-wire ion chamber (MWIC).

Consisting of two wire planes (vertical and horizontal), each with 10 wires, the MWIC measures the incident beam position and profile both prior to and after patient positioning, to verify that the beam properties did not change. The beam stop immediately after the MWIC prevents treatment until the beam properties are verified. Three 1 mm thick plastic viewing scintillators aid the operator in the initial tuning of the beam. The upstream collimator has four segments (left, right, up, down) with a current readout for each segment at the operator's console. The collimator's 1 cm diameter aperture is sufficient to allow 100% beam transmission, yet protect the patient in the event of a gross beam deflection. Once the beam is properly tuned, each segment should read less than 0.1 nA. After passing through the segmented collimator opening, the beam is visible on the second viewing scintillator, which is mounted on the support for the first scattering foil.

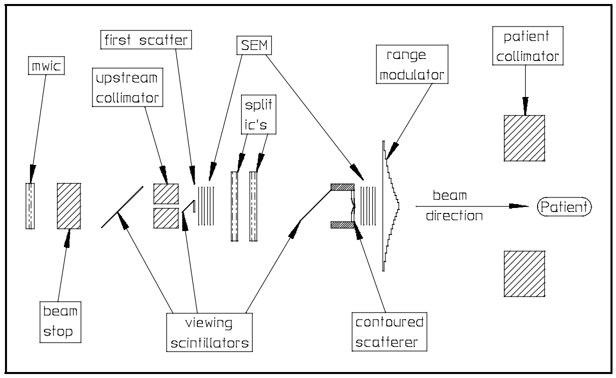

Figure 1 Schematic layout of the proton therapy beam line. (Not to scale).

This scattering foil is part of the lateral beam spreading system, necessary to provide large, uniform dose distributions. We have tested a system which uses two scattering foils and an occluding-ring assembly,[2] as well as one using an initial scattering foil followed by a contoured scattering foil [3] (as shown in Figure 1). For each case, the geometry was calculated using the Harvard beam spreading program NEU.[3] A typical dose profile is shown in section V of this paper.

The first secondary electron emission monitor (SEM) [4] is located immediately after the first scattering foil. Each SEM is constructed of 11 mylar foils, aluminized on both sides and glued with conductive epoxy to copper clad PC board rings stacked on three rods. Every other foil is biased at +100 V and collects electrons knocked out of the unbiased foils. The unbiased foils are connected to a current integrator.

The SEM is used to measure total beam current as well as dose delivered. Initially the SEM is calibrated with a Faraday cup to obtain an absolute beam intensity measurement. For dose delivery, the SEM is calibrated against a Markus ion chamber. The Markus chamber, manufactured by Nuclear Associates, is cross-calibrated with a Farmer type cylindrical ion chamber (model NEL 2505/3A) which has been calibrated at K&S Associates, an accredited dosimetry laboratory.

Both SEMs have been calibrated over the full range of intensities available to the proton therapy beam line and have a very linear response. Unlike ion chambers, they are not susceptible to saturation at high beam currents, a condition that may exist while beam splitting at low duty factors. There is no measurable difference in dose delivered between continuous 100% duty cycle beam and beam from the beam splitter at 10% duty cycle.

After the first SEM are two split ion chambers. Each of these has two planes, one split vertically, and one split horizontally. These monitor the symmetry of the beam intensity, with two for redundancy. The symmetry of the beam intensity is quite sensitive to the incident beam position and trajectory at the first scattering foil. Those are the only parameters that can affect the dose distribution from this passive scattering system, so by monitoring these ion chambers we can be confident that our lateral dose distribution is uniform to better than 10%.

Further downstream is the contoured scattering foil, which is mounted in a collimator with the third viewing scintillator on the upstream side of the collimator. Immediately after the second scattering foil is the second SEM.

The next element of our beam line is an acrylic range modulator,[5] which is used to modulate the range of the Bragg peak. Several range modulators have been constructed, giving modulation from 3 to 18 cm (depth in water). A computer program [6] calculated the physical characteristics of the range modulator, given the measured (unmodulated) Bragg peak data.

At the end of our beam line is a patient chair. Because this is a fixed horizontal beam, we will be treating head, neck, and brain tumors. The patient chair has a fixture to immobilize a patient's head. The chair has 5 degrees of freedom (height, lateral, longitudinal, rotation about the vertical axis, and a tilt motion), with digital readouts for each. To assist in accurate positioning, there are fixed laser beams, a light field, and a portable x-ray unit for port verification films. A collimator to restrict the field to the treatment region is mounted just upstream from the patient.

IV. <u>ELECTRONICS</u>

Our control system is part of the new IUCF system,[7] which is based on the commercial Vista software running on a VAX. The I/O interface is VME [8] based, with all signals entering our system through one of two types of VME modules: either a Matrix combination ADC/DAC/PIO board (MD-DAADIO) or a LeCroy 1151 scaler. These modules are read through the VME bus by an AEON rt300 VAX (which is also a VME module). The rt300 processes the incoming signals, and communicates in several ways. Some devices receive instructions from the rt300 via the output channels of the MD-DAADIO board. Other information is distributed via the rt300's ethernet connection. Both raw and processed signals can be graphically display and monitored on an independent X-Window station.

Current signals from the MWIC, each SEM, and each section of the split ion chambers are converted to logic pulses whose frequency is proportional to the incoming signal. This is done in a module designed and built by our group. A high sensitivity version was designed and constructed to handle the typically small signals from the SEMs. These have a sensitivity of 10 pC. A more economical model with a sensitivity of 1 nC is used for the signals from the MWIC and split ion chambers (which have inherent gains of the order of 100).

The pulses from these devices are counted using the LeCroy 1151 scalers. Since the dose calibration of the SEMs ultimately relates collected charge to dose, every time the computer reads the scaler module, the cumulative dose delivered is known. Reading these modules does not disable their counting function, nor is there the dead-time typically associated with analog-to-digital conversion. This technique allows us to continuously measure the total dose delivered.

Another important feature of the 1151 scaler modules is that they are bi-directional, and provide a signal after counting down from a preset value. While one scaler is counting the total dose delivered, another is counting down from the prescribed dose (+ 3%). If the computer system should fail to stop the beam by reading that the prescribed dose has been reached, the scaler will provide a front panel logic signal indicating a dose excess of 3%. This signal is hardwired to an independent system which will interrupt the beam by shutting off the ion source. Each SEM is connected to a separate scaler module, so that there are redundant safety systems.

The remaining signals are monitored through the MD-DAADIO board. These include all of the bias voltages, as well as signal levels indicating the position of the beam stop and the scattering foils, and a signal from a motion sensor on the range modulator. Through an output channel of the MD-DAADIO board, the rt300 provides a continuous signal if it determines that all inputs meet the "status OK". If the signal from some device is inconsistent with the "status OK" condition, or if the rt300 itself fails, the MD-DAADIO output signals drops, which stops the beam. In addition, the radiation oncologist can stop the beam via the computer system from the X-Window station, or via a mechanical button which is part of the IUCF radiation safety system.

A few devices are using existing electronics. A Brookhaven Instruments Corp. model 1000C current integrator is used to read the Faraday cup, and a Keithley model 614 integrating electrometer is used to read charge collected by the Markus ion chamber. Each of these devices also provides an output signal which is incorporated into the computer system. Dose calibrations are then done automatically by the computer, but can be independently verified by the digital readouts on those electronics. (Although the physicists still rely on hand calculators.) Finally, dose distributions are measured using a water phantom and a stand-alone Multidata computer dosimetry system.

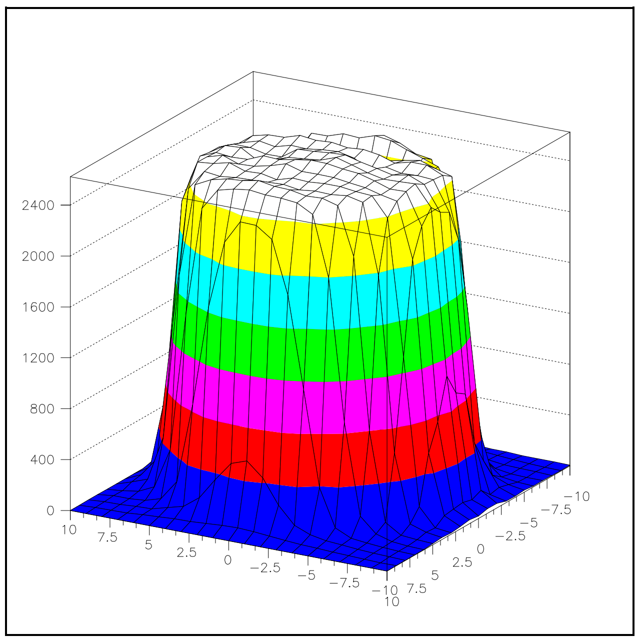

Figure 2 Lateral beam profile shows proton dose (arbitrary units) distribution as a function of horizontal and vertical position (in cm).

V. MEASUREMENTS

Beam profiles were measured with the Multidata water phantom for different field sizes, different beam energies, and using 2 different types of passive scattering systems. Under all situations satisfactory results were obtained. Figure 2 shows a profile taken with a nominally 20 cm field and a 15 cm diameter collimator immediately upstream of the water phantom. The incident beam energy was 200 MeV, and the beam was spread using the occluding-ring type spreading system. Table I summarizes the measured fields, giving the field size defined by the location at which the dose drops by 5%, the average dose uniformity within the actual field size, and the penumbra ($P_{90\text{-}50}$) at various depths. The occluding-ring type spreading systems were used initially because of their ease of manufacture. While satisfactory performance was obtained, we expect to use a contoured scattering foil system for patient

Table I: Beam Profile Results

Size (cm)	Flatness (%)	Symmetry (%)	Penumbra (cm)
18.6	1.6	1	2.2
11.9	2.6	2	1.9
8.5	1.5	1	1.8

Field **size** is the distance between the 95% points on a beam profile ionization curve, normalized to the central axis value.

Flatness is the variation in ionization profile, measured over the central 80% of the field.

Symmetry is the deviation from 1 of the maximum ratio of ionization readings (averaged over 1 cm) for symmetric points in the flat (central 80%) region of an ionization profile.

Penumbra is the distance between the 90% and 10% ionization points

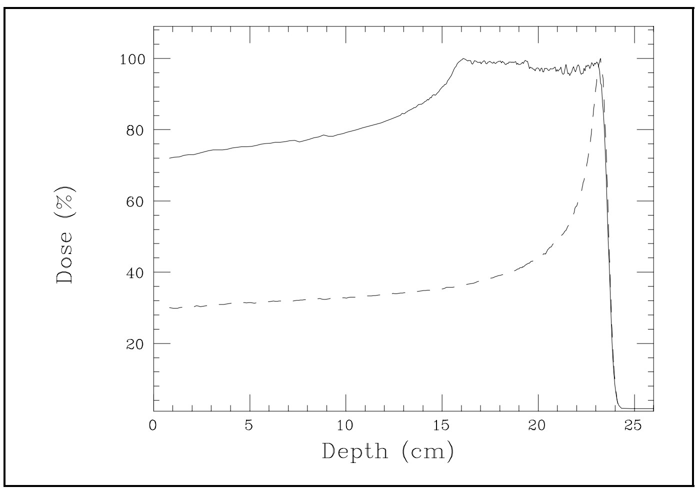

Figure 3 Bragg peak without range modulation, superimposed on a SOBP with a 7.4 cm plateau.

treatments, because the resulting beam profile is less sensitive to error in the incident beam trajectory.

A typical 200 MeV Bragg peak and a 7.4 cm spread out Bragg peak (SOBP) are shown in Figure 3. Table II gives the measured SOBP characteristics which have been obtained so far. Improvements in the range modulator design program have led to excellent flatness (generally less than 3% deviation). Further work needs to be done to minimize the distal falloff, although present values (< 0.7 cm for 200 MeV beam) are sufficient for many treatments.

Table II: Depth Modulation Results

Modulation (cm)	Surface Dose (%)	Flatness (%)	Distal Falloff (cm)
4.3	59	4.6	.67
7.5	71	2.8	.65
19.0	95	3.3	.70

Modulation is the extant of the depth plateau.

Surface dose is the ratio of the ionization measured near the surface to that measured at the peak.

Flatness is defined similar to that for the profile.

The **distal falloff** is the distance from the 90% ionization level to the 10% ionization level at the distal edge.

The RBE of the proton beam, as compared to ^{60}Co radiation, was assessed by observing several parameters in DBA/2J mice following total body irradiation in a uniform field.[9] The parameters observed were LD_{100}, spleen cell cellularity, lymphocyte proliferation, and frequency of chromatin fragment formation. Table III summarizes the results, where the error bars represent the statistical uncertainties. Previously published data [10][11][12][13][14] show a significant spread in RBE values for high energy protons. Our own data indicate a dose (or possibly a dose rate) dependence. Because of these uncertainties, we will adopt the conservative (and clinically tested) value of 1.10 for the proton RBE.

VI. SUMMARY

The IUCF proton beam is well matched to the demands of proton therapy in available intensity and energy. The beam splitting system allows proton therapy work to continue with little impact to the ongoing basic research program. The beam spreader and range modulator produce beams suitable for proton therapy and measurements of efficiency of beam use will be made. The dose uniformity is sufficient both in depth and transverse to the beam direction and the penumbra is reasonable. We have produced a wide range of field sizes and flat SOBP's. The SEMs and split ion chambers provide reliable measurements of delivered dose. We can reliably position patients for treatment of head, neck, and brain tumors. The next available beam will be used for several practice treatments using a humanoid phantom. After satisfactory results are obtained from those tests, patient treatments will begin.

Table III: Summary of RBE Values Measured

Biological Endpoint	Dose (cGy)		
	150	400	800
LD_{100}	---	---	1.27±0.04
Spleen Cell Cellularity	1.38±0.25	1.32±0.50	1.36±0.29
Lymphocyte Proliferation	1.08±0.04	1.34±0.04	1.10±0.40
Frequency of Chromatin Fragment Formation	1.22±0.26	1.31±0.11	1.26±0.12
Average	1.09±0.04	1.34±0.04	1.27±0.04

VII. THE FUTURE

Our highest priority is to complete the final system tests, and commence patient treatments. Once that is underway, several projects will be considered which would provide obvious benefits. The first is the installation of a fourth Lambertson magnet, which would allow us to split beam between the Cooler ring and the proton therapy beam line.

A second area of development is raster scanning of the beam (instead of a passive spreading system). We have scanning magnets and power supplies available which have passed initial beam tests. We would need to develop a control system specific to raster scanning, but the DC nature of the cyclotron beam makes that task less difficult than with typical time structures of synchrotron beams.

Ultimately, we hope to go beyond a fixed beam line. Since our present treatment room is too small for any type of gantry system, we have begun to investigate the feasibility of constructing a new treatment room and extending the beam line to that area.

VIII. ACKNOWLEDGEMENTS

We wish to thank the Lions Cancer Control Fund of Indiana and Lions International for their generous financial support.

IX. REFERENCES

[1] D.L Friesel, T. Ellison, and T. Sloan, IUCF Scientific and Technical Report, 142 (1986).

[2] A.M. Koehler, R.J. Schneider, and J.M. Sisterson, Med. Phys. **4**, 297 (1977).

[3] B. Gottschalk, Harvard Cyclotron Lab internal report HCL 3/23/90 (1990).

[4] G.W. Tautfest and H.R. Fechter, Rev. Sci. Inst. **26**, 229 (1955).

[5] A.M. Koehler, R.J. Schneider, and J.M. Sisterson, Nucl. Instrum. Meth. **131**, 437 (1975).

[6] C. Bloch *et al.*, Indiana University Proton Therapy internal report (unpublished).

[7] John Collins, IUCF Scientific and Technical Report, 223 (1992).

[8] Versa Module Europa (VME) bus is defined by the IEEE 1014-1987 standard.

[9] R-N. Shen, G.A. Sandison, C. Bloch, W.N. Crabtree, V. Derenchuk, M. Fasano, N.B. Hornback, H. Shidnia, and P. Young, to be published (1992).

[10] E.J. Hall, D. Phil, A.M. Kellerer, H.H. Rossi, and Y-M. Lam, Int. J. Radiat. Oncol. Biol. Phys., **4**, 1009 (1978).

[11] J.B. Robertson, J.R. Williams, R.A. Schmidt, J.B. Little, D.F. Flynn, and H.D. Suit, Cancer **35**, 1644 (1975).

[12] J. Tepper, L. Verhey, M. Goitein, H.D. Suit, and D. Phil, Int. J. Radiat. Oncol. Biol. Phys. **2**, 1115 (1977).

[13] M. Urano, M. Goitein, L. Verhey, O. Mendiondo, H.D. Suit, and A. Koehler, Int. J. Radiat. Oncol. Biol. Phys. **6** 1187 (1980).

[14] M. Urano, L. Verhey, M. Goitein, J.E. Tepper, H.D. Suit, D. Phil, O. Mendiondo, E.S. Gragoudas, and A. Koehler, Int. J. Radiat. Oncol. Biol. Phys. **10** 509 (1983).